

## Airborne sound transmission modeling of walls based on random point process theory

Cédric VAN HOORICKX and Edwin P.B. REYNDERS

KU Leuven, Department of Civil Engineering, Belgium, cedric.vanhoorickx@kuleuven.be

### Abstract

A novel approach is presented to compute the diffuse sound transmission through modally sparse walls. The fact that the natural frequencies in the adjacent rooms can be considered to form a sequence of random points on the frequency axis makes this problem amenable to analysis by random point process theory. The method makes use of the fact that for any diffuse subsystem the local spacings between the eigenvalues saturate to those of a Gaussian orthogonal ensemble (GOE) matrix and the statistics of its mode shapes saturate to Gaussian random fields, with a spatial covariance function depending only on wavelength and distance. This stochastic modelling approach is computationally very efficient and is illustrated for a calcium silicate block wall and a gypsum block wall.

Keywords: Random point process theory, Airborne sound transmission, Diffuse field

### 1 INTRODUCTION

In a measurement setup, the airborne sound insulation of a partitioning wall is subject to many sources of uncertainty. These are often difficult to quantify due to lack of information or model complexity. At high frequencies, the sound pressure at a specific location in the room is sensitive to local variations of the acoustic field properties caused by random wave scattering inside and at the boundaries of the source and receiver room. Usually a diffuse field approach is considered, which is a random field, composed of a large number of statistically independent plane waves with a uniformly distributed spatial phase.

When the local sound pressure in the room is highly sensitive to local variations of the acoustic field properties, it can be modeled as a pure-tone diffuse reverberant field, as in Statistical Energy Analysis (SEA). In this approach, the system is decomposed into homogeneous subsystems whose response is characterized with a single random variable, namely its total energy. Next to the mean of the total sound energy over the random ensemble of rooms, also the variance can be predicted [4], employing a non-parametric model of uncertainty. In many applications, some of the subsystems of a built-up system are very sensitive to small wave scatterers, while others are not. In this mid-frequency range, a hybrid method can be used combining deterministic and stochastic energy based methods. This has been achieved in the hybrid FE-SEA approach [10], based on a reciprocity relationship that links the mean vibrational energy of a non-parametric random SEA subsystem to the variance of the nodal forces at its boundary.

This paper presents a novel approach to compute the airborne sound insulation of walls. The same assumptions are made as for a hybrid FE-SEA approach, namely that (1) the wave field of each random subsystem across the random ensemble can be assumed diffuse and (2) the mode shapes saturate to Gaussian fields. Instead of directly computing the ensemble mean and variance of the total energy, the approach presented here uses a Monte Carlo simulation, where every sample represents a realization of the diffuse subsystem. An advantage of this procedure is that parametric uncertainty in the modally sparse subsystems can be easily included by also varying the uncertain parameters in every Monte Carlo realization. This is useful in e.g. assessing the reproducibility of a measurement procedure using a virtual round robin test [12]. The approach utilizes the random point process theory, which relies on the assumption that the natural frequencies can be considered to form a sequence of random points on the frequency axis. This assumption is only valid the natural frequencies mix with respect to each other across the random ensemble of rooms, which is the case at high frequencies.

## 2 PREDICTION MODEL FOR AIRBORNE SOUND INSULATION

The problem considered in this paper is the airborne sound transmission through a modally sparse wall in between two diffuse rooms. Quantities related to the source room are indicated with subscript 1, quantities related to the wall with subscript 2, and quantities related to the receiver room with subscript 3.

### 2.1 System of equations

The transmission loss is computed using the assumed-modes method, approximating the pressure fields of the source room  $p_1$  and receiver room  $p_3$  and the vibration field of the wall  $u_2$  into a finite set of basis functions:

$$p_{1/3} \approx \sum_{i=1}^{n_{1/3}} \phi_{1/3i}(x, y, z) q_{1/3i}(\omega) = \boldsymbol{\phi}_{1/3} \mathbf{q}_{1/3} \quad u_2 \approx \sum_{j=1}^{n_2} \phi_{2j}(y, z) q_{2j}(\omega) = \boldsymbol{\phi}_2 \mathbf{q}_2 \quad (1)$$

Inserting these approximations into Lagrange's equations of motion and adopting a hysteretic damping model yields the following linear system of equations:

$$\begin{bmatrix} \mathbf{D}_{11} & \mathbf{K}_{12} & \mathbf{0} \\ \mathbf{K}_{21} & \mathbf{D}_{22} & \mathbf{K}_{23} \\ \mathbf{0} & \mathbf{K}_{32} & \mathbf{D}_{33} \end{bmatrix} \begin{Bmatrix} \mathbf{q}_1 \\ \mathbf{q}_2 \\ \mathbf{q}_3 \end{Bmatrix} = \begin{Bmatrix} \mathbf{f}_1 \\ \mathbf{0} \\ \mathbf{0} \end{Bmatrix} \quad (2)$$

where

$$\mathbf{D}_{kk} = -\omega^2 \mathbf{I}_k + \boldsymbol{\Omega}_k^2 (1 + i\eta_k) \quad (3)$$

with  $i$  the imaginary unit and  $\boldsymbol{\Omega}_k$  the diagonal matrix containing the circular undamped eigenfrequencies for subsystem  $k$  corresponding to the mode shapes in  $\boldsymbol{\phi}_k$ . The damping loss factors of the rooms are computed from their reverberation times via  $\eta = 4.4\pi/(\omega T)$ . A point monopole with volume acceleration  $a_p(\omega)$  is assumed, located at  $(x_p, y_p, z_p)$ . Element  $i$  of the loading vector  $\mathbf{f}_1$  then reads

$$f_{1i}(\omega) = -\rho_a a_p(\omega) \phi_{1i}(x_p, y_p, z_p) \quad (4)$$

The matrices  $\mathbf{K}_{12}$  and  $\mathbf{K}_{32}$  are coupling matrices that represent the loading on the room due to the plate movement, and  $\mathbf{K}_{21}$  and  $\mathbf{K}_{23}$  represent the loading on the plate due to the room pressure. The elements of the coupling matrices are:

$$K_{21,ji} = \int_0^{L_{y2}} \int_0^{L_{z2}} \phi_{1i}(L_{x1}, y, z) \phi_{2j}(y, z) dz dy \quad K_{12,ij} = -\rho_a \omega^2 K_{21,ji} \quad (5)$$

$$K_{23,jk} = \int_0^{L_{y2}} \int_0^{L_{z2}} \phi_{3k}(L_{x1}, y, z) \phi_{2j}(y, z) dz dy \quad K_{32,kj} = -\rho_a \omega^2 K_{23,jk} \quad (6)$$

### 2.2 Computation of the sound reduction index

In order to efficiently solve equation (2), row reduction is performed on the block matrices to reduce the size of the system of equations in equation (2). This yields:

$$\mathbf{A} \mathbf{q}_2 = \mathbf{b} \quad (7)$$

where the elements of the matrices  $\mathbf{A}$  and  $\mathbf{b}$  are given by:

$$A_{mn} = D_{22,mn} + \rho \omega^2 \sum_{i=1}^{n_1} \frac{K_{21,mi} K_{21,ni}}{D_{11,ii}} + \rho \omega^2 \sum_{k=1}^{n_3} \frac{K_{23,mk} K_{23,nk}}{D_{33,kk}} \quad b_m = -\sum_{i=1}^{n_1} \frac{K_{21,mi} f_{1i}}{D_{11,ii}} \quad (8)$$

The energy in the source and receiver room can then be computed as:

$$E_1 = \frac{1}{\rho_a} \sum_{i=1}^{n_1} \frac{\left| f_{1i} - \sum_{j=1}^{n_2} K_{12,ij} q_{2j} \right|^2}{|D_{11,ii}|^2} \approx \frac{1}{\rho_a} \sum_{i=1}^{n_1} \frac{|f_{1i}|^2}{|D_{11,ii}|^2} \quad E_3 = \rho_a \omega^4 \sum_{k=1}^{n_3} \frac{\left| \sum_{j=1}^{n_2} K_{23,jk} q_{2j} \right|^2}{|D_{33,kk}|^2} \quad (9)$$

The sound reduction index  $R$  is finally computed with the measurement formula:

$$R = 10 \log_{10} \left( \frac{E_1}{V_1} \right) - 10 \log_{10} \left( \frac{E_3}{V_3} \right) + 10 \log_{10} \left( \frac{S_2}{A_3} \right) \quad (10)$$

in which  $V_1$  and  $V_3$  are the volume of the source and receiver room,  $S_2$  is the surface area of the partition, and  $A_3$  is the absorption of the receiver room.

### 3 SUBSYSTEM PROPERTIES

The computations require the natural frequencies and mode shapes of the subsystems to be computed. The rooms are modeled as diffuse subsystems, the wall is assumed to be a deterministic subsystem.

#### 3.1 Deterministic subsystem

If the wall can be modeled as a homogeneous, isotropic, thin plate, its natural frequencies are given by:

$$\omega_{2j} = \sqrt{\frac{D_2}{m_2''} \left[ \left( \frac{m_{jy}\pi}{L_{y2}} \right)^2 + \left( \frac{m_{jz}\pi}{L_{z2}} \right)^2 \right]} \quad (11)$$

with  $D_2$  the bending stiffness,  $m_2''$  the mass of the wall per unit area,  $L_{y2}$  the width, and  $L_{z2}$  the height of the wall. The integers  $m_{jy}$  and  $m_{jz}$  represent the number of half wavelengths in the plate dimensions. The mode shapes of the wall are calculated as follows:

$$\phi_{2j} = \frac{2}{\sqrt{m_2'' L_{y2} L_{z2}}} \sin \left( \frac{m_{jy}\pi y}{L_{y2}} \right) \sin \left( \frac{m_{jz}\pi z}{L_{z2}} \right) = A_2 \sin(k_{2jy} y) \sin(k_{2jz} z) \quad (12)$$

#### 3.2 Diffuse subsystems

The wave fields in the rooms are modeled as diffuse fields. Diffuse field models essentially describe rooms with locally uncertain geometric properties, material properties, and/or boundary conditions, that is, rooms with uncertain wave scatterers. The mode shapes of a room in high-frequency regime can be interpreted as standing waves that arise from many traveling plane wave components. Adopting a diffuse acoustic field model, the pressure mode shape at a given location consists of a summation of independent plane acoustic waves with the same mean amplitude and uncorrelated phases, coming from all directions with equal probability. It then follows from the central limit theorem that the acoustic mode shapes are zero-mean, Gaussian random fields. A zero-mean Gaussian random field is uniquely determined by its covariance function.

For diffuse reflecting boundaries, the mode shapes  $\phi_{si}$  are statistically homogenous, i.e., the statistics of the pressure mode shape components are independent of their position. The corresponding random wave field is a diffuse field. For three-dimensional volumes, its covariance function then has the form [1]:

$$\mathbf{C}_{si}(\mathbf{x}, \mathbf{x}') = \begin{cases} A_s j_0(k_{si} |\mathbf{x} - \mathbf{x}'|) & \text{for 2 points inside the room, away from a deterministic boundary} \\ 2A_s j_0(k_{si} |\mathbf{x} - \mathbf{x}'|) & \text{for 2 points on a reflecting boundary, away from joints and corners} \end{cases} \quad (13)$$

where  $j_0(x) = \sin(x)/x$  is the spherical Bessel function of the first kind and order zero,  $k_{si} := \frac{2\pi}{\lambda_{si}}$  denotes the wavenumber corresponding to the wavelength  $\lambda_{si}$  of mode  $i$  for subsystem  $s$ , and  $A_s$  is a factor that is independent of position, which can be determined from the mode shape normalization condition. In an acoustic

enclosure  $\Omega$  with volume  $V_s$ , the normalization condition reads:

$$\int_{\Omega} \frac{1}{c^2} \phi_{si}^2(\mathbf{x}) d\mathbf{x} = 1 \quad \Leftrightarrow \quad A_s = \frac{c^2}{V_s}. \quad (14)$$

The correlation function (13) depends only on the distance between the considered mode shape components, the wavelength and the total volume. Close to perfectly reflecting boundaries, the mean squared sound pressure equals twice the mean squared sound pressure in the center of the room [13]. Because of this, a factor two appears in the covariance function (13) for points located on the reflecting structural element. In addition, when the distance between  $\mathbf{x}$  and  $\mathbf{x}'$  is large compared to the wavelength  $\lambda_{si}$ , it follows from the above expressions that the mode shapes evaluated at these distinct points are approximately uncorrelated.

### 3.3 Computation of the coupling matrices

Instead of numerically evaluating the integrals in equations (5) and (6), the statistics of the coupling matrices are computed directly. When integrating a Gaussian field, it is the limit of a linear combination of Gaussian random variables so it is again Gaussian. The entries of the coupling matrix are therefore Gaussian variables and are determined by their mean and variance. As the mean of the mode shapes in the rooms equals zero, also the mean of the coupling matrices equals zero. The variance of  $K_{21,kl}$  is computed as follows:

$$\text{Var}(K_{21,ji}) = \iiint \iiint E[\phi_{1i}(L_{x1}, y, z) \phi_{1i}(L_{x1}, y', z')] \phi_{2j}(y, z) \phi_{2j}(y', z') dz' dz dy' dy \quad (15)$$

The term  $E[\phi_{1i}(L_{x1}, y, z) \phi_{1i}(L_{x1}, y', z')]$  is the covariance function for two points on a reflecting boundary (equation (13)), and this integral becomes:

$$\text{Var}(K_{21,ji}) = 2A_1 A_2^2 \iiint \iiint j_0(k_{1i}|\mathbf{x} - \mathbf{x}'|) \sin(k_{2jy}y) \sin(k_{2jy}y') \sin(k_{2jz}z) \sin(k_{2jz}z') dz' dz dy' dy \quad (16)$$

where the integrals go from 0 to  $L_{y2}$  for the ones in  $y$  and  $y'$  and from 0 to  $L_{z2}$  for the ones in  $z$  and  $z'$ . The distance function in the spherical Bessel function is given by  $|\mathbf{x} - \mathbf{x}'| = \sqrt{(y - y')^2 + (z - z')^2}$ . The quadruple integral can be converted into the following double integral:

$$\text{Var}(K_{21,ji}) = 2A_1 A_2^2 L_{y2}^2 L_{z2}^2 \int_0^1 \int_0^1 j_0(a_{1iy} \sqrt{u^2 + \gamma^2 v^2}) h(a_{2jy}, u) h(a_{2jz}, v) dv du \quad (17)$$

with  $a_{1iy} = k_{1i} L_{y2}$ ,  $\gamma = L_{z2}/L_{y2}$ ,  $a_{2jy} = k_{2jy} L_{y2}$ ,  $a_{2jz} = k_{2jz} L_{z2}$ , and:

$$h(a, u) = (1 - u) \cos(au) - \frac{\cos(a)}{a} \sin(a(1 - u)) \quad (18)$$

The integral in equation (17) is evaluated numerically. The mean and variance of  $K_{23,jk}$  is computed in the same way.

## 4 RANDOM POINT PROCESS THEORY

### 4.1 Introduction

Note that for obtaining the energies in the rooms, sums are needed over expressions with  $D_{11,kk}$  or  $D_{33,kk}$  in the denominator, i.e. in Eqs. (8) and (9). At high frequencies, the computation cost of the sound reduction index is dominated by these sums. The natural frequencies can be considered to form a sequence of random points on the frequency axis, and thus the problem is amenable to analysis by random point process theory [11]. Strictly, the natural frequency point process is assumed to be stationary, which is only the case if the modal density of

the subsystems is constant, and this is not true in this case. On the other hand, only a limited number of modes significantly contribute at any considered frequency. As the modal density is approximately constant over the frequency range corresponding to these modes, it is reasonable to assume that the point process is stationary.

A distinction is made between type 1 and type 2 sums, with type 1 referring to the sums in Eq. (8) and type 2 referring to the ones in Eq. (9). The terms of these sums have  $D_{11,kk}$  or  $D_{33,kk}$  in the denominator. From the definition of the matrices  $D_{11,kk}$  and  $D_{33,kk}$ , the type 1 sums  $S_1(\omega)$  and type 2 sums  $S_2(\omega)$  can be expressed as:

$$S_1(\omega) = \sum_k \frac{c_k}{-\omega^2 + \omega_k^2(1+i\eta)} \quad S_2(\omega) = \sum_k \frac{c_k}{|-\omega^2 + \omega_k^2(1+i\eta)|^2} = \sum_k \frac{c_k}{(\omega_k^2 - \omega^2)^2 + \eta^2 \omega_k^4} \quad (19)$$

Unless  $c_k$  is much smaller at  $\omega \approx \omega_k$  than at other frequencies, it follows that the modes mainly contributing to the summations are the ones in the vicinity of the considered frequency. These sums can also be written as:

$$S_1(\omega) = \int_{-\infty}^{\infty} h_1(\omega, \omega') \xi(\omega') d\omega' \quad S_2(\omega) = \int_{-\infty}^{\infty} h_2(\omega, \omega') \xi(\omega') d\omega' \quad (20)$$

where

$$\xi(\omega') = \sum_k c_k \delta(\omega' - \omega_k) \quad (21)$$

$$h_1(\omega, \omega') = \frac{1}{-\omega^2 + \omega'^2(1+i\eta)} \approx \frac{1}{2\omega} \frac{\omega' - \omega - i\omega\eta/2}{(\omega' - \omega)^2 + (\eta\omega/2)^2} \quad (22)$$

$$h_2(\omega, \omega') = \frac{1}{(\omega'^2 - \omega^2)^2 + \eta^2 \omega'^4} \approx \frac{1}{4\omega^2} \frac{1}{(\omega' - \omega)^2 + (\eta\omega/2)^2} \quad (23)$$

in which the approximations are commonly used [3, 5].

Random point process theory now allows computing the statistics of these sums. These are separately discussed for the two sum types in the next to subsections.

## 4.2 Statistics of type 1 sums

Weaver [14] found that, for the generic case where the considered spatial uncertainty does not preserve symmetries, the statistics of the local eigenvalue spacings saturate to those of the Gaussian Orthogonal Ensemble (GOE) matrix from random matrix theory [7]. It can be shown that the GOE assumption leads to the following statistics (more precisely the ensemble mean and variance) of the type 1 sum  $S_1(\omega)$  as defined in (20) [5]:

$$\mathbb{E}[S_1(\omega)] = -\frac{i\mathbb{E}[c_k] \pi n}{2\omega} \quad \text{Var}(\text{Re}\{S_1(\omega)\}) = \text{Var}(\text{Im}\{S_1(\omega)\}) = \frac{\pi n}{4\omega^3 \eta} \mathbb{E}[c_k]^2 \left( \alpha - 1 + \frac{1}{\pi m} \right) \quad (24)$$

where  $n$  is the modal density,  $m = \omega\eta n$  the modal overlap factor and  $\alpha = \mathbb{E}[c_k^2] / \mathbb{E}[c_k]^2$ .

As for diffuse subsystems, these sums are performed over many modes, it is assumed, according to the central limit theory, that the real and imaginary part of the sums have a Gaussian distribution. This is for example consistent with the assumption of Schroeder [9] that transfer functions written in the form of a modal sum, which are closely related to the type 1 sums<sup>1</sup>, are approximately complex Gaussian. A realization of a type 1 sum is therefore obtained from:

$$S_1(\omega) = -\frac{i\mathbb{E}[c_k] \pi n}{2\omega} + (\xi_R + i\xi_I) \sqrt{\frac{\pi n}{4\omega^3 \eta} \mathbb{E}[c_k]^2 \left( \alpha - 1 + \frac{1}{\pi m} \right)} \quad (25)$$

<sup>1</sup>The similarity between the type 1 sums and the transfer function in modal form can be easily seen by comparing Eq. (19) and the transfer function expression e.g. in [5]: the denominator of the sum terms is the same, the numerator consists of the product of two zero-mean Gaussian factors

with  $\xi_R$  and  $\xi_I$  realizations of normally distributed random numbers with mean 0 and standard deviation 1. The only terms still to be determined are the mean and mean of the square of the factors  $c_k$  for the sums in (8). These are calculated from basic probability rules:

$$E[K_{21,mi}K_{21,ni}] = \sigma_{K_{21,m}}^2(\omega)\delta_{mn} \quad E[(K_{21,mi}K_{21,ni})^2] = (2\delta_{mn} + 1)\sigma_{K_{21,m}}^2(\omega)\sigma_{K_{21,n}}^2(\omega) \quad (26)$$

$$E[K_{21,mif1i}] = 0 \quad E[(K_{21,mif1i})^2] = \sigma_{K_{21,m}}^2(\omega)\sigma_{f1i}^2 = \frac{\rho^2 c^2}{V_1}\sigma_{K_{21,m}}^2(\omega) \quad (27)$$

in which  $\sigma_{K_{21,m}}^2(\omega) = \text{Var}\left(K_{21,mi}\left(k_{1i} = \frac{\omega}{c}\right)\right)$ .

### 4.3 Statistics of type 2 sums

The mean and variance of type 2 sums equal [2, 3]:

$$E[S_2(\omega)] = \frac{E[c_k]\pi n}{2\eta\omega^3} \quad \text{Var}(S_2(\omega)) = E[S_2(\omega)]^2 \left( \frac{\alpha - 1}{\pi m} + \frac{1}{(\pi m)^2} \right) \quad (28)$$

The type 2 sums appear in Eq. (9), which represent the total energies in the source and receiver room. As the total energy of a subsystem is empirically found to follow a log-normal distribution [6], also the sums appearing in Eq. (9) are assumed to have a log-normal distribution. A realization of a type 2 sum is therefore obtained as follows. First the mean  $\mu_2$  and standard deviation  $\sigma_2$  of the natural logarithm are computed:

$$\mu_2(\omega) = \ln \left( \frac{E[S_2(\omega)]}{\sqrt{1 + \frac{\text{Var}(S_2(\omega))}{E[S_2(\omega)]^2}}} \right) \quad \sigma_2^2(\omega) = \ln \left( 1 + \frac{\text{Var}(S_2(\omega))}{E[S_2(\omega)]^2} \right) \quad (29)$$

after which a realization is obtained from

$$S_2(\omega) = \exp(\mu_2(\omega) + \xi\sigma_2(\omega)) \quad (30)$$

with  $\xi$  a realization of a normally distributed random number with mean 0 and standard deviation 1.

For the sums in Eq. (9), the mean and mean of square of the factors  $c_k$  are given by:

$$E[|f_{1i}|^2] = \sigma_{f1i}^2 E[\xi_{1i}^2] = \frac{\rho^2 c^2}{V_1} \quad E[|f_{1i}|^4] = \sigma_{f1i}^4 E[\xi_{1i}^4] = 3\frac{\rho^4 c^4}{V_1^2} \quad (31)$$

$$E \left[ \left| \sum_{j=1}^{n_2} K_{23,jk} q_{2j} \right|^2 \right] = \sum_{j=1}^{n_2} \sigma_{K_{23,j}}^2(\omega) |q_{2j}|^2$$

$$E \left[ \left| \sum_{j=1}^{n_2} K_{23,jk} q_{2j} \right|^4 \right] = \left( \sum_j |q_{2j}|^2 \sigma_{K_{23,j}}^2(\omega) \right)^2 + 2 \sum_i \sum_j \text{Re} \{ q_{2i} q_{2j}^* \}^2 \sigma_{K_{23,i}}^2(\omega) \sigma_{K_{23,j}}^2(\omega) \quad (32)$$

In summary, the ensemble probability distribution of the sound reduction index  $R$  is obtained as follows. A Monte Carlo simulation is performed in which each sample represents a realization of the system. In each sample, realizations of the sums in Eq. (8) are computed using Eq. (25), after which the system of equations in Eq. (7) is solved to obtain the vibration field of the wall  $\mathbf{q}_2$ . The energies in the source and receiver room are then computed from Eq. (9), in which realizations of the sums are computed from Eq. (30). Finally, the sound reduction index is computed with the measurement formula in Eq. (10).

## 5 APPLICATIONS

In this section, the proposed method is applied to compute the airborne sound insulation of a calcium silicate block wall and a gypsum block wall. A total of 1000 Monte Carlo realizations are computed. The approach from this paper is compared with two other approaches: a deterministic model, where the sound field in the emitting and receiver rooms are expanded as a sum of their hard-walled modes, and the hybrid FE-SEA approach as presented in [8]. In all computations, the source and receiver rooms have a volume of  $87\text{m}^3$  and a reverberation time of 1.5s. The wall size is  $3 \times 3.3\text{m}^2$ .

First, a heavy single-leaf wall is studied. The wall has a thickness of 25cm and consists of calcium silicate blocks with mass density  $\rho = 1800\text{kg/m}^3$ , Young's modulus  $E = 10.8\text{GPa}$ , and Poisson's ratio  $\nu = 0.2$ . The mean of the predicted sound transmission loss and the corresponding 95% confidence interval are shown in Fig. 1a. The dips in the insertion loss correspond to the individual wall modes, indicating that, especially at low frequencies, the modal density of the wall is generally low ( $n = 0.0274\text{modes/Hz}$ ). The critical frequency of the wall is at 102.5Hz, yet no clear coincidence dip is observed because of the low modal density. Above the critical frequency, the transmission loss increases with approximately 9dB per octave. The presented approach corresponds almost perfectly with the hybrid FE-SEA approach.

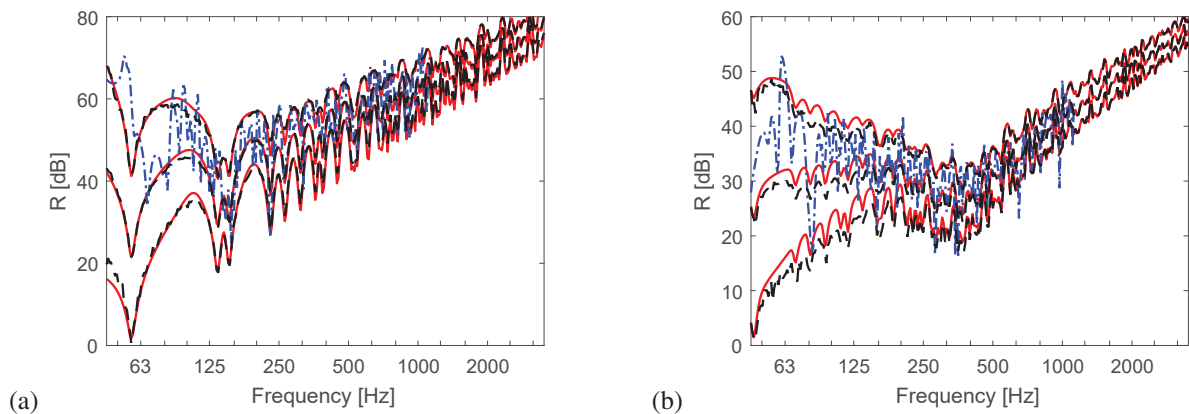


Figure 1. Mean and 95% interval of the sound reduction index for (a) the calcium silicate wall and (b) the gypsum block wall computed using three approaches: deterministic approach (blue dash-dotted line), hybrid FE-SEA approach (red solid line), and the approach presented in this paper (black dashed line).

The second example is a lightweight single-leaf wall with a thickness of 10cm. It consists of gypsum blocks with mass density  $\rho = 910\text{kg/m}^3$ , Young's modulus  $E = 3.15\text{GPa}$ , and Poisson's ratio  $\nu = 0.2$ . The mean of the predicted sound transmission loss and the corresponding 95% confidence interval are shown in Fig. 1b. In contrast to the heavy wall from the previous section, no clear dips are observed in the harmonic transmission loss statistics, as the modal density is higher ( $n = 0.0899\text{modes/Hz}$ ). A clear coincidence dip is observed around the critical frequency of 334.2Hz, behind which the transmission loss increases with approximately 9dB per octave. Also for this case, a good correspondence with the hybrid FE-SEA approach is obtained, especially at high frequencies.

## 6 CONCLUSIONS

In this paper, a novel approach is presented to compute the airborne sound transmission through a wall located between two diffuse rooms. The approach is therefore a hybrid approach, coupling the deterministic structural subsystem with the random acoustic subsystems. The computation of the airborne sound transmission is performed through a Monte Carlo simulation, in which each sample corresponds to a realization of the random ensemble. The natural frequencies in the diffuse rooms are considered to form a sequence of random points

on the frequency axis, which makes this problem amenable to analysis by random point process theory. The approach furthermore uses the fact that for any diffuse subsystem the mode shapes saturate to Gaussian random fields, with a covariance function depending only on wavelength and distance. Two applications are presented, a calcium silicate block wall and a gypsum block wall. For both applications, the presented approach shows good correspondence with the hybrid FE-SEA approach.

## ACKNOWLEDGEMENTS

The research presented in this paper has been performed within the frame of the VirBAcoustics project (project ID 714591) “Virtual building acoustics: a robust and efficient analysis and optimization framework for noise transmission reduction” funded by the European Research Council in the form of an ERC Starting Grant. The financial support is gratefully acknowledged.

## REFERENCES

- [1] R. Cook, R. Waterhouse, R. Berendt, S. Edelman, and M. Thompson Jr. Measurement of correlation coefficients in reverberant sound fields. *Journal of the Acoustical Society of America*, 27(6):1072–1077, 1955.
- [2] R. Langley and A. Brown. The ensemble statistics of the band-averaged energy of a random system. *Journal of Sound and Vibration*, 275(3–5):847–857, 2004.
- [3] R. Langley and A. Brown. The ensemble statistics of the energy of a random system subjected to harmonic excitation. *Journal of Sound and Vibration*, 275(3–5):823–846, 2004.
- [4] R. Langley and V. Cotoni. Response variance prediction in the statistical energy analysis of built-up systems. *Journal of the Acoustical Society of America*, 115(2):706–718, 2004.
- [5] R. Langley and V. Cotoni. The ensemble statistics of the vibrational energy density of a random system subjected to single point harmonic excitation. *Journal of the Acoustical Society of America*, 118(5):3064–3076, 2005.
- [6] R. Langley, J. Legault, J. Woodhouse, and E. Reynders. On the applicability of the lognormal distribution in random dynamical systems. *Journal of Sound and Vibration*, 332(13):3289–3302, 2013.
- [7] M. Mehta. *Random Matrices*. Elsevier, San Diego, CA, 3rd edition, 2004.
- [8] E. Reynders, R. Langley, A. Dijkmans, and G. Vermeir. A hybrid finite element - statistical energy analysis approach to robust sound transmission modelling. *Journal of Sound and Vibration*, 333(19):4621–4636, 2014.
- [9] M. Schroeder. Statistical parameters of the frequency response curves of large rooms. *Journal of the Audio Engineering Society*, 35(5):299–306, 1987.
- [10] P. Shorter and R. Langley. Vibro-acoustic analysis of complex systems. *Journal of Sound and Vibration*, 288(3):669–699, 2005.
- [11] R. Stratonovich. *Topics in the theory of random noise*, volume I. Gordon and Breach, New York, NY, 1963.
- [12] C. Van hoorickx and E. Reynders. Uncertainty quantification of sound transmission measurement procedures based on the Gaussian Orthogonal Ensemble. In D. Herrin, J. Cuschieri, and G. Ebbitt, editors, *Proceedings of the 47th International Congress and Exposition on Noise Control Engineering, Inter-Noise 2018*, Chicago, USA, August 2018. CD-ROM.
- [13] R. Waterhouse. Interference patterns in reverberant sound fields. *Journal of the Acoustical Society of America*, 27(2):247–258, 1955.
- [14] R. Weaver. On the ensemble variance of reverberation room transmission functions, the effect of spectral rigidity. *Journal of Sound and Vibration*, 130(3):487–491, 1989.